The Journal of Experimental Biology 211, 1376-1385
Published by The Company of Biologists 2008
doi:10.1242/jeb.015941

Retinal processing and opponent mechanisms mediating ultraviolet polarization sensitivity in rainbow trout (*Oncorhynchus mykiss*)

Samuel D. Ramsden[1], Leslie Anderson[1], Martina Mussi[1], Maarten Kamermans[2,3] and Craig W. Hawryshyn[1,*]

[1]Department of Biology, University of Victoria, PO Box 3020 STN CSC, Victoria, British Columbia, V8W 3N5, Canada, [2]Retinal Signal Processing Group, Netherlands Institute for Neuroscience, Meibergdreef 47, 1105 BA Amsterdam, The Netherlands and [3]Department of Neurogenetics, Academic Medical Center, University of Amsterdam, Meibergdreef 9, 1105 AZ Amsterdam, The Netherlands

*Author for correspondence at present address: Department of Biology, Center for Neuroscience Studies, Queen's University, Kingston, Ontario, K7L 3N6, Canada (e-mail: craig.hawryshyn@queensu.ca)

Accepted 19 February 2008

SUMMARY

A number of teleost fishes have photoreceptor mechanisms to detect linearly polarized light. We studied the neuronal mechanism underlying this ability. It was found that a polarized signal could be detected in rainbow trout (*Oncorhynchus mykiss*) both in the electroretinogram (ERG) and in the compound action potential (CAP) measured in the optic nerve, indicating a strong retinal contribution to the processing of polarized light. The CAP recordings showed a W-shaped sensitivity curve, with a peak at 0°, 90° and 180°, consistent with processes for both vertical and horizontal orientation. By contrast, the ERG recordings reveal a more complex pattern. In addition to the peaks at 0°, 90° and 180°, two additional peaks appeared at 45° and 135°. This result suggests a specialized contribution of the outer retina in the processing of polarized light. The spectral sensitivity of the mechanisms responsible for these intermediate peaks was studied using chromatic adaptation. Here we show that long wavelength-sensitive (LWS) cone mechanism adaptation shifted the intermediate peaks towards 90°, whereas ultraviolet-sensitive (UVS) cone mechanism adaptation shifted the peaks away from 90° towards either 0° or 180°. These results provide further confirmation that the 90° peak is dominated by the LWS cone mechanism and the 0° and 180° peaks are dominated by the UVS cone mechanism. In addition, a pharmacological approach was used to examine the retinal neural mechanisms underlying polarization sensitivity. The effect of blocking negative feedback from horizontal cells to cones on the ERG was studied by making intraocular injections of low doses of cobalt, known to block this feedback pathway. It was found that the intermediate peaks seen in the ERG polarization sensitivity curves were eliminated after application of cobalt, suggesting that these peaks are due to outer retinal inhibition derived from feedback of horizontal cells onto cones. A simple computational model was developed to evaluate these results. The model consists of opponent and non-opponent processing elements for the two polarization detectors. This model provides a first approximation analysis suggesting that opponent processing occurs in the outer retina for polarization vision. Although it seems that polarization vision uses a slightly more complicated coding scheme than colour vision, the results presented in this paper suggest that opponent and non-opponent channels process polarization information.

Key words: ultraviolet, polarization sensitivity, electrophysiology, fish, cobalt, horizontal cell, electroretinogram, compound action potential.

INTRODUCTION

The visual world of fish is a complex environment, where colour, intensity and polarization of light are available to guide behaviours (Cronin and Shashar, 2001; Parkyn et al., 2003; Novales Flamarique and Hawryshyn, 1997; McFarland and Munz, 1975a; Pomozi et al., 2001). The complexity of the underwater photic environment is mirrored by the diversity of visual adaptations that have evolved to perceive these qualities of light (Barry and Hawryshyn, 1999; McFarland and Munz, 1975b; Novales Flamarique and Hawryshyn, 1993). Many species of fish have evolved visual mechanisms for the perception of linearly polarized light and behaviours based on this perception, such as spatial orientation behaviour for either laboratory or natural illumination experiments (Hawryshyn and McFarland, 1987; Hawryshyn et al., 2003; Parkyn and Hawryshyn, 2000; Parkyn et al., 2003; Mussi et al., 2005; Shashar and Cronin, 1996; Shashar et al., 1998; Shashar et al., 2001; Shashar and Hanlon, 1997; Waterman and Hashimoto, 1974).

Biophysical models have been proposed to explain the selective absorption of electric-vector (e-vector) orientations of polarized light in vertebrate photoreceptors (Novales Flamarique et al., 1998; Roberts et al., 2004; Roberts and Needham, 2007). The proposed models for e-vector absorption include: (i) internal reflection within double cones onto neighbouring ultraviolet-sensitive (UVS) cones resulting from the partitioning membrane and the geometry of the cone mosaic (Novales Flamarique et al., 1998; Allison et al., 2003); (ii) axial dichroism of cone photoreceptors through tilting of the outer segment disc membranes (Roberts et al., 2004; Roberts and Needham, 2007).

A number of techniques have been used to examine polarization sensitivity (PS) in several teleost species including: heart rate conditioning (Hawryshyn and McFarland, 1987), single unit recording from the torus semicircularis (Coughlin and Hawryshyn, 1995) and the optic tectum (Waterman and Hashimoto, 1974), compound action potential (CAP) recordings from the optic nerve

(Parkyn and Hawryshyn, 1993; Parkyn and Hawryshyn, 2000), electroretinograms (ERGs) (Hawryshyn et al., 2003) and behavioural orientation and discrimination paradigms (Hawryshyn et al., 1990; Parkyn et al., 2003; Degner and Hawryshyn, 2001; Mussi et al., 2005). However, examinations of the neuronal pathways underlying PS have been restricted to several species of cyprinids and salmonids. These studies have mainly employed techniques such as single unit recording techniques in the torus semicircularis and CAP recording techniques in the optic nerve (for a review, see Hawryshyn, 2000).

CAP recordings by Parkyn and Hawryshyn (Parkyn and Hawryshyn, 1993; Parkyn and Hawryshyn, 2000) identified horizontal and vertical polarization detector mechanisms by examining the PS of the four cone mechanisms isolated through chromatic adaptation. Chromatic adaptation is a technique that uses spectral backgrounds to selectively depress cone mechanisms, usually resulting in the isolation of one cone mechanism's sensitivity [see Hawryshyn and McFarland (Hawryshyn and McFarland, 1987) for an illustration of this technique]. Briefly, these experiments, like those performed on goldfish (Hawryshyn and McFarland, 1987), demonstrated that the UVS cone mechanism mediated vertical PS, whereas the medium and long wavelength-sensitive (MWS and LWS) cone mechanisms mediated horizontal PS. When a spectrally broad background is used in conjunction with UV linearly polarized stimuli, PS curves show a 'W-shaped' PS function. Peak PS occurs at 0° and 90°, representing the combined presence of the vertical and horizontal polarization detector mechanisms. A full description of these observations is provided in Parkyn and Hawryshyn (Parkyn and Hawryshyn, 1993) and Coughlin and Hawryshyn (Coughlin and Hawryshyn, 1995). In a recent study, we examined PS of three species of damselfishes (three-spot damselfish, *Dascyllus trimaculatus*; blacktail damselfish, *D. melanurus* and blue-green chromis, *Chromis viridis*) using ERG recordings (Hawryshyn et al., 2003). The non-invasive nature of the technique made it an attractive methodology for measuring PS and doing so repeatedly in the same individual. The observed PS from ERG recordings was more complex (four peaks) than the two-channel W-function commonly found in salmonids using CAP recording. ERG evaluation of PS in salmonids had not been previously attempted. Studies that have used ERG recording to measure PS in vertebrates such as pigeons have resulted in conflicting results, largely because of methodological issues such as avoiding the measurement of UV polarization sensitivity and because of incorrect interpretation of ERG data (Kreithen and Keeton, 1974; Delius et al., 1976; Hzn et al., 1995).

The overall purpose of the work presented here was to explore where in the retina critical coding steps may occur for polarization vision. The sensitivity to polarized light was determined at two locations: (1) at the output stage of the retina, by recording CAPs in the optic nerve (late stage processing), and (2) at the input stage of the retina, by recording the ERG (early stage processing). Using chromatic adapting backgrounds, the spectral sensitivity of the various components of the responses was determined and using a pharmacological approach, the nature of the underlying neuronal mechanism was studied. Here we show that critical polarization processing takes place in both the outer and inner retina. Short and long wavelength chromatic adaptation predictably displaced the angular position of the intermediary peaks in ERG PS curves relative to the peak vertical and horizontal detector mechanisms by changing the weighting of opponent interactions. Cobalt injections, which are known to block feedback of horizontal cells on cones, resulted in an elimination of the intermediary peaks in ERG PS curves. The presence of these intermediary peaks in ERG PS curves and their absence in CAP PS strongly implicates a special role of the outer retina in processing linearly polarized light.

MATERIALS AND METHODS

Animals and holding conditions

Juvenile rainbow trout (*Oncorhynchus mykiss* Walbaum) of 5–10 g body mass were obtained from the Fraser Valley Trout Hatchery, Abbottsford, British Columbia, Canada. Fish were held on a 12 h:12 h L:D photoperiod and maintained at 15±1°C. All surgical procedures were conducted between 08:00 h and 18:00 h to avoid any effects related to diel retinomotor movements (Parkyn and Hawryshyn, 1993; Parkyn and Hawryshyn, 2000). The photic conditions within the holding facility were provided by full spectrum fluorescent lamps (6500 K). All experimental procedures and animal care were approved by the University of Victoria Animal Care Committee, under the auspices of the Canadian Council for Animal Care.

Preparation of fish

Experimental preparations for both electroretinograms (ERGs) and compound action potential (CAP) recordings are described elsewhere in detail (Beaudet et al., 1993; Hawryshyn et al., 2003; Parkyn and Hawryshyn, 2000). In brief, rainbow trout were immersed in a solution of 125 mg l^{-1} tricane methanesulphonate (MS-222) until the fish reached stage IV anaesthesia (Joly et al., 1972). Standard length (cm) and body mass (g) were measured. Subcuteaneous injections of a general anaesthetic, Maranil (0.005 mg kg^{-1} body mass) and an immobilizing agent, pancuronium bromide (0.05 mg g^{-1} body mass) were administered at several sites. The test fish were then placed in a holding cradle in a Faraday cage. Experimental fish were irrigated with aerated fresh water (10°C, flow rate of approximately 3 ml s^{-1}) and the body covered with a moist cloth. For CAP experiments, the dermis overlying the right frontal bone was removed with a scalpel and surgical drill, holding a dental burr. This provided access to the right rostral optic tectum through which the recording electrode was advanced into the optic nerve.

Experimental apparatus

The optical system and recording apparatus have been described previously (Hawryshyn et al., 2003; Parkyn and Hawryshyn, 2000). Two background channels using 250 W quartz-halogen lamps (Ushio Cypress, CA, USA) were used to provide constant background fields and chromatic adaptation. Long and short wavelength cut-off interference filters, Schott colour filters and neutral density filters/wedge, were used to manipulate both the energy and wavelength distribution of each background channel. A quantum catch model was employed to determine filter combinations necessary to produce the desired background conditions (Table 1). A bifurcated fibre optic (fused silica, n.a.=0.22; Fiberoptic Systems

Table 1. Quantum capture calculations for background adaptation conditions

	Quantum catch (photons cm^2 s^{-1})			
	UVS cones	SWS cones	MWS cones	LWS cones
Control	3.92×10^{10}	3.69×10^{11}	2.06×10^{12}	3.89×10^{12}
LWS cone adapting	3.92×10^{10}	3.69×10^{11}	2.45×10^{12}	1.09×10^{13}
UVS cone adapting	5.27×10^{10}	4.19×10^{11}	2.19×10^{12}	4.04×10^{12}

LWS, long wavelength sensitive; MWS, medium wavelength sensitive; SWS, short wavelength sensitive; UVS, ultraviolet sensitive.

Inc., Simi Valley, CA, USA) was used to superimpose the background channels onto the eye. The stimulus channel used a 300 W xenon arc lamp system (Thermo Oriel, Stratford, CT, USA). The optical path consisted of a monochrometer (Instruments SA), Inconel quartz neutral density wedge (0–4.0 neutral density; Melles-Griot, Rochester, NY, USA), shutter (Uniblitz, Vincent Associates, Rochester, NY, USA), optical filters to block spectral sidebands, and UV optics to match the numerical aperture of the liquid light pipe (n.a.=0.74). The stimulus and background illuminated the left eye of the fish. Both the stimulus and background fields were spatially broad, to mimic natural presentation of celestial and underwater-polarized light. Spectral sensitivity was measured in 20 nm increments, from 360 to 620 nm, using a staggered wavelength presentation to prevent adaptation to a certain region of the spectrum.

For PS measurements, a UV-transmissive linear polarizer (HNP'B, Polaroid Corporation, Concord, MA, USA; manually adjusted) was placed over the ferrule of the liquid light pipe. Measurements were randomized, from 0° to 180°, in 15° increments, where the 0°/180° e-vector axis was defined as vertical relative to the gravitational axis of the fish and 90/270° was defined as horizontal (Hawryshyn and McFarland, 1987). Fish were light adapted with unpolarized light from the background channels, and a plane-polarized, 360 nm stimuli, in 0.2 log unit increment steps, was used to measure UV PS. The use of two light pipes, one for the stimulus and the other for the background eliminated e-vector adaptation from the background channel. A quantum catch model was used to generate photic conditions aimed at carefully controlling the level of light adaptation of the respective cone mechanisms:

$$Q_i = \int A_i(\lambda)G(\lambda)d(\lambda)\,, \qquad (1)$$

where Q_i denotes the quantum catch of receptor (i), $A_i(\lambda)$ denotes the visual pigment absorption coefficient of receptor (i), a $G(\lambda)$ denotes the photon irradiance (spectral energy distribution) of the background light field and $d(\lambda)$ denotes wavelength (nm). Integrations were performed for each receptor mechanism, between 300 and 800 nm, for the various background conditions considered. This assessment, in addition to cone mechanism light adaptation dynamics (Hawryshyn, 1991), allowed us to finely control the state of adaptation of the cone mechanisms. Such considerations were essential to avoid complete suppression of either the UVS or LWS cone mechanisms. The following background adaptation conditions were used: (i) white light background – 700 nm short pass (SP; Coherent Inc., Santa Clara, CA, USA; also used in ii and iii) plus 2.0 neutral density filters (Coherent Inc.; also used in ii and iii) in each background channel (1 and 2); (ii) LWS cone mechanism adaptation – 600 nm long pass (LP; Coherent Inc.; cut-off filter) and 1.5 neutral density in channel 1, and 700 nm SP and 2.0 neutral density filters in background channel 2; (iii) UVS cone mechanism adaptation – UG-11 (Shott filter) and 1.3 neutral density filters in channel 1, and 700 nm SP and 2.0 neutral density filters in channel 2. Spectral energy distribution curves are shown in Fig. 1.

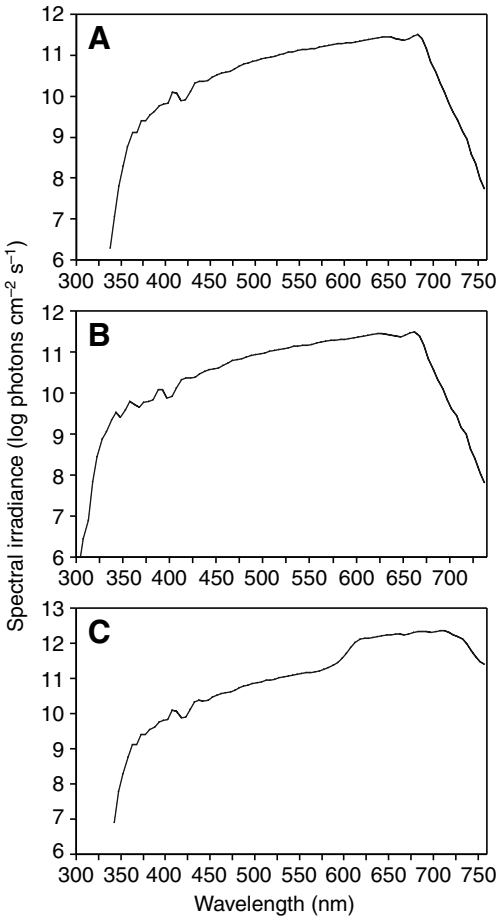

Fig. 1. Spectral energy distribution of the adapting backgrounds. The irradiance measurements are plotted as log irradiance (photons cm^2 s^{-1}). (A) Broad-spectrum tungsten halogen adapting background used in control and cobalt PS and spectral sensitivity experiments. (B) UVS cone mechanism, adapting background using a UG-11 filter in a tungsten halogen background channel. (C) LWS cone mechanism, adapting background using a 600LP cut-off filter.

Intraocular injections

Existing research has shown that sub-millimolar concentrations of cobalt (50–100 μM) block the horizontal cell feedback of cones in turtles (Thoreson and Burkhardt, 1990; Vigh and Witkovsky, 1999) and in fish (Fahrenfort et al., 2004). Injections of either cobalt chloride (Sigma-Aldrich) or saline were made at the limbus of the left eye using a 30-gauge needle. Final concentrations of cobalt were estimated following the method used by Demarco and Powers (Demarco and Powers, 1989). In short, the average volume of the vitreous was estimated to be 145 μl, and 10 μl of 4.26 mmol l^{-1} cobalt was injected, resulting in an estimated final ocular concentration of 0.275 mmol l^{-1}. These concentrations represent first order approximations of the cobalt chloride concentration in the eye. These values may not reflect what is actually present in the outer retina at the time of our measurements (i.e. these values are likely overestimates). For instance, our estimates of the concentration of cobalt chloride may not be directly comparable to those in an isolated retina or eyecup preparations superfused with physiological medium and pulsed with cobalt chloride.

Recording procedure: electroretinogram (ERG)

A glass electrode [1 mm i.d., loaded with saline (28 p.p.t. sodium chloride)] was inserted into a saline filled half-cell (A-M systems Inc., Carlsborg, WA, USA), and the tip was positioned using a micromanipulator on the dorsal-nasal surface of the left eye. A ground electrode was attached to the caudal fin and a chlorided-silver reference electrode was placed in the right nares of the test fish. Fish were acclimated for 45 min prior to experiments using chromatic adaptation or cobalt treatments. A Grass Hi-Z probe (Grass-Telefactor probe, Grass Instruments, West Warwick, RI, USA) provided the input to a Grass instruments P-5 preamplifier

(bandpass filter settings, 0.3 Hz low-pass and 300 Hz high-pass). The amplified signal was analyzed with a 16-bit A/D data acquisition board (National Instruments, Inc., Austin, TX, USA). A custom-designed software analysis module determined the b-wave amplitude by measuring the change in potential from the peak a-wave to peak b-wave, during the period 150 ms post stimulus onset. The stimulus duration was 500 ms with an inter-stimulus interval of 20 s.

Compound action potential (CAP)

A sharpened Teflon-coated chlorided-silver electrode (0.5 mm diameter, 0.5 mm exposed tip) was inserted into the optic nerve of the left eye using a micromanipulator, following procedures used by Parkyn and Hawryshyn (Parkyn and Hawryshyn, 1993; Parkyn and Hawryshyn, 2000). Correct placement of the recording electrode into the optic nerve was crucial, since Coughlin and Hawryshyn (Coughlin and Hawryshyn, 1995) demonstrated that optic tecta do not possess UV polarization-sensitive neurons. To avoid misplacement of the recording electrode, a custom-designed stereotaxic apparatus was used. Further, the waveform recorded in response to photic stimuli differs between tectal and optic nerve location of the electrode tip (see Parkyn and Hawryshyn, 2000). *Post mortem* dissections verified the correct trajectory and placement of the electrode. Ground and reference electrodes were placed on the fish as described above.

The amplitude of the onset response of the optic nerve compound action potential was determined by comparing the baseline noise amplitude 50 ms prior to stimulus onset with the response amplitude 50 ms post stimulus onset.

Analysis of electroretinograms and optic nerve responses

Response *versus* intensity (RI) curves for each wavelength and e-vector combination were generated and statistically fitted with a third order polynomial function. A criterion response was selected to intersect within the linear dynamic range of the RI curve and normally set at 20 μV above the base line noise for ERG and 50 μV above baseline noise for CAP. Threshold intensities were interpolated from RI curves using the 20 μV (Fig. 2D) and 50 μV (Fig. 2C) above baseline response criterion. Threshold intensity values were normalized between 0 and 1 to remove differences in absolute sensitivity between individuals.

The model

The input signals for the model are described by Eqn (2) and (3) and were taken as the logarithmic response of polarization amplitude detected:

$$V = \log_{10}[\cos^2(\alpha)], \quad (2)$$

$$H = \log_{10}[\sin^2(\alpha)], \quad (3)$$

where, V and H denote the response of the vertical and horizontal detector mechanisms, α is the polarization angle of the incident light. A linear subtractive model was used to examine the opponent interactions between the V and H polarization detector mechanisms:

$$S_v = (k_1 V) - (k_2 H), \quad (4)$$

$$S_h = (k_3 H) - (k_4 V), \quad (5)$$

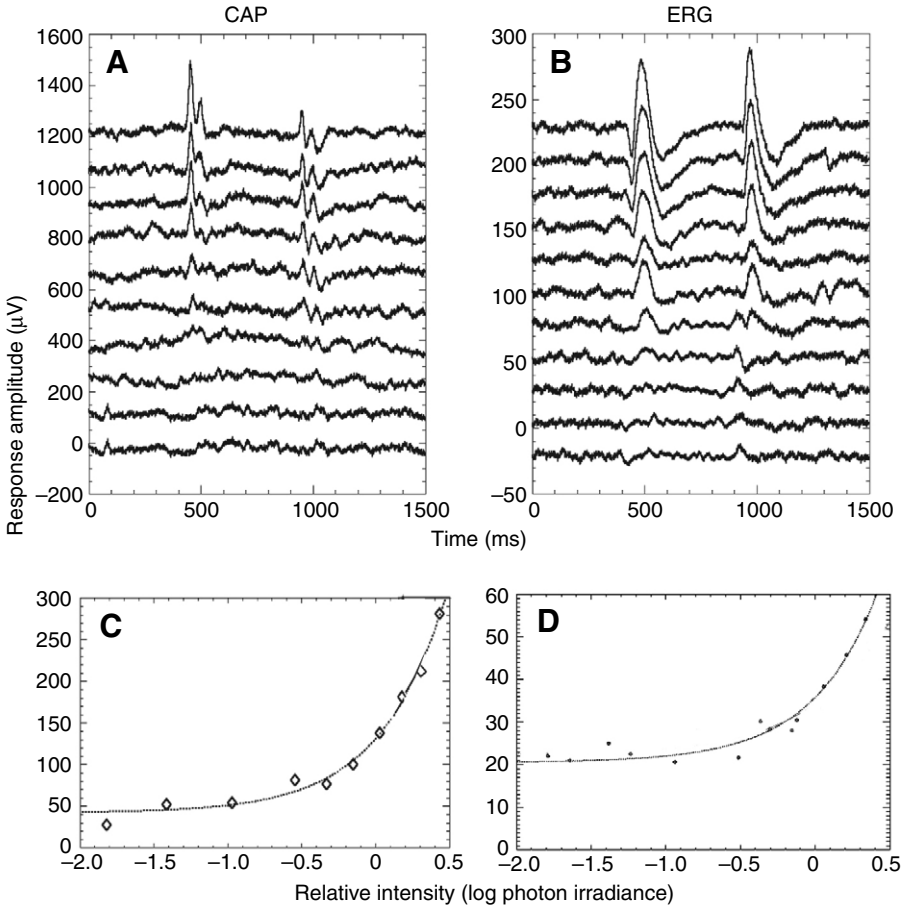

Fig. 2. Waveforms and response *versus* intensity curves for compound action potential (CAP) and electroretinogram (ERG) recording. (A) CAP waveforms ('ON' responses) at increasing intensities. Note that individual traces for A and B were vertically displaced for clarity of presentation. Intensity was incremented in 0.2 log unit steps of a 360 nm linearly polarized stimulus with an e-vector orientation of 45°. (B) ERG waveforms at increasing intensities recorded from a control fish (sham control, intraocular injection of saline). (C) Response *versus* intensity curve based on CAP data taken from panel A. (D) Response *versus* intensity curve based on ERG data taken from B.

Table 2. Weighting factors for computations using the linear subtractive model (Eqns 4 and 5)

Condition	Weighting factors			
	k_1	k_2	k_3	k_4
CAP Fig. 4A	0.75	1.6	1.5	0.9
ERG Fig. 4B	0.8	7.0	6.0	0.9
600 LP adaptation Fig. 5A	0.6	2.0	8.0	0.85
UG-11 adaptation Fig. 5B	0.75	8.0	2.0	0.85
Cobalt Fig. 8A	0.78	5.0	5.0	0.7
Saline Fig. 8B	0.75	1.6	1.5	0.8

CAP, compound action potential; ERG, electroretinogram; LP, long pass.

where, S_v is the sensitivity (0–1 on a normalized scale) of the vertical detector mechanism with the amplitude of inhibitory influence of V and H set by weighting factors k_1 and k_2, and S_h is the sensitivity of the horizontal mechanism (0–1 on a normalized scale) with the amplitude of inhibitory influence of V and H set by weighting k_3 and k_4 (see Table 2).

RESULTS

ERG and CAP responses to 500 ms flashes of 360 nm linearly polarized light were determined for a number of intensities (Fig. 2). Intensity response curves were constructed and the intensities required to produce a criterion response of 20 μV above baseline for ERG and 50 μV above baseline for CAP were determined. The reciprocal of the threshold intensity was defined as sensitivity. Fig. 2A shows the CAP responses for various intensities. The waveforms have been vertically displaced for presentation clarity and represent responses to 0.2 log unit increments in stimulus intensity, with the lowest intensity at the base of the plot. The CAP recordings from the optic nerve shown in Fig. 2A were comparable to those observed in our previous studies (e.g. Parkyn and Hawryshyn, 2000). Optic nerve recording waveforms exhibited responses at light onset and offset. The onset response amplitudes were plotted against stimulus intensity to illustrate the response dynamics of ganglion cell axons in the optic nerve. The response *versus* intensity curve shown in Fig. 2C was described by a third order polynomial expression. Threshold intensity was estimated using a criterion response set at 50 μV above baseline and interpolating the stimulus intensity. The ERG recordings shown in Fig. 2B share the same graphical format as Fig. 2A. At higher intensities, the control ERG waveforms show the classical components [a-, b-, c- and d-waves (Brown, 1968)]. The intensity response relationship is given in Fig. 2D with the dashed line representing a third order polynomial fit. For these recordings the threshold criterion was set at an amplitude of 20 μV above baseline.

To study the contribution of the various cone systems to the vertical and the horizontal polarization mechanisms, chromatic adaptation experiments were performed. First, we tested whether the chromatic adapting backgrounds had the expected effect on the

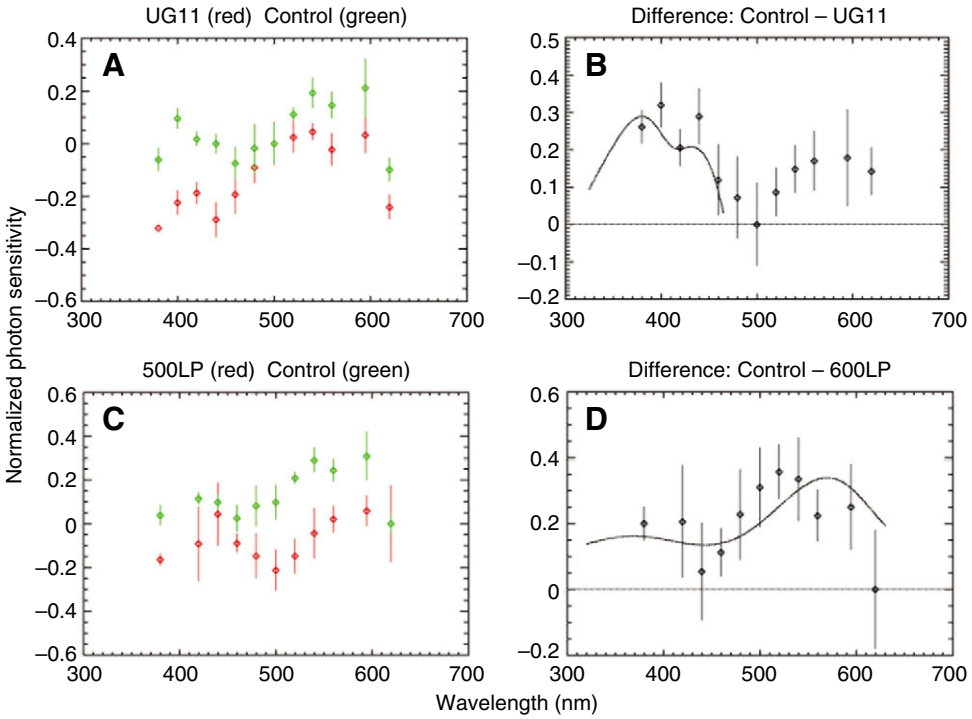

Fig. 3. Mean normalized spectral sensitivity of rainbow trout (±1 standard error) using electroretinogram (ERG) recording. For each treatment condition, panels on the left side show the spectral sensitivity curves for the control and treatment conditions and the panels on the right side show the difference curves between the control and treatment spectral sensitivity. Green points represent the control and red points represent the treatment condition. The sensitivity measurements were normalized to 360 nm. (A) Mean normalized spectral sensitivity of control fish where the spectral sensitivity was measured using a broad-spectrum tungsten halogen background (N=3), and treatment fish where spectral sensitivity was measured using a broad spectrum and UG-11 background (N=3). (B) Mean difference spectrum as a result of short wavelength chromatic adaptation (UG-11 filter). The black line fitted to the data points at the shortwave end of the spectrum represents an additive function based on the UVS and short wavelength-sensitive (SWS) visual pigment templates. (C) Mean normalized spectral sensitivity of the same control fish as in A, and treatment fish where spectral sensitivity was measured using a broad spectrum and 600 nm long pass background (N=3). (D) Mean difference spectrum as a result of long wavelength chromatic adaptation (600 nm long pass filter). The black line fitted to the points represents the LWS cone visual pigment template.

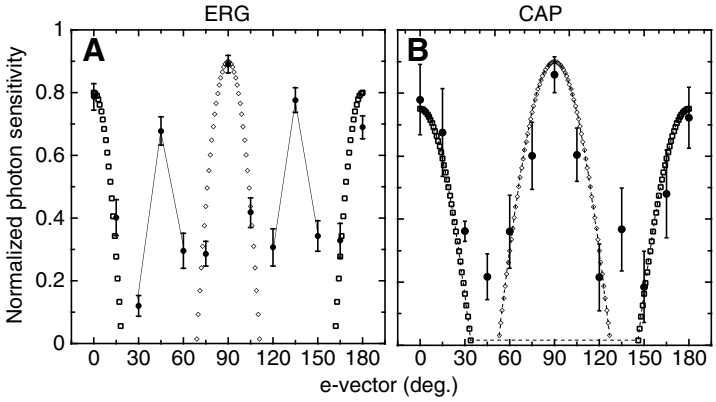

Fig. 4. Mean ultraviolet polarization sensitivity of rainbow trout (±1 standard error). Two different recording techniques were used, electroretinogram (ERG) and compound action potential (CAP) recording (solid circles). S_v is represented by squares and S_h by diamonds (see Table 2 for weighting coefficients). Dashed lines connect the symbols. (A) ERG PS (N=21). The solid line connects the sensitivity points representing the intermediary peaks. (B) CAP PS (N=5). For both figures, a 360 nm linear polarized stimulus in 15° e-vector increments was used. Note the differences in sensitivity between the two curves at 45° and 135°.

spectral sensitivity of the ERG and the CAP responses. Fig. 3 shows, as expected, that UVS cone mechanism adaptation leads to a reduction of the sensitivity in the short wavelength part of the spectrum and that LWS cone mechanism adaptation leads to a reduction of sensitivity in the long wavelength part of the spectrum. It is critical to note that both the adapting backgrounds were adjusted to exert relatively minor changes in the adaptational state of cone mechanisms, since the overall modulation amplitude in polarization sensitivity is relatively small (i.e. less than 1 log unit). However, the difference spectra demonstrate that changes in cone mechanism sensitivity were nonetheless detectable.

Next we examined the effect of these adapting backgrounds on PS. If we compare UV PS for CAP and ERG recording techniques, the CAP response has its characteristic W-shape whereas the ERG has intermediate peaks at 45° and 135° (Fig. 4). The peaks for the ERG are all equally sized. Although a small secondary peak at 135° could also be seen in the CAP response, the secondary peaks are a prominent feature of the ERG and very minor in the CAP. Since the CAP response has been described in detail elsewhere, we will focus for the rest of the paper on the ERG responses. The model was fit to all polarization tuning curves. The open squares represent the model fit for the vertical system (S_V) and the open diamond symbols represent the horizontal system (S_H). Similar model traces are shown in Fig. 5A,B. The model fits show that chromatic adaptation influences the breadth or angular bandwidth of both the vertical and horizontal detector mechanisms. When a longwave background (600 nm longpass) was used the horizontal detector mechanism narrowed and the vertical mechanism broadened. The opposite was observed when a UV background (UG-11) was used.

Previously, we determined that the vertical polarization detector was dominated by the UVS cone mechanism, whereas the horizontal polarization detector was dominated by the LWS cone mechanism. If the intermediate peaks were due to an opponent interaction between these two polarization mechanisms, chromatic adaptation would lead to a shift of the intermediate peak away from the more sensitive cone mechanism or polarization detector. This prediction was confirmed in Fig. 5A. Under 600 LP chromatic adaptation, the peak of the ERG profile shifted from 45° and 135° (Fig. 4A) to 60 and 120°, respectively. Similarly, chromatic adaptation with UG-11 (UV chromatic adaptation) shifts the peaks in the opposite direction towards the vertical detector mechanism (Fig. 5B).

Next the site of this inhibition was studied. Sub-milimolar concentrations of Co^{2+} are known to inhibit feedback from horizontal cells to cones. An intraocular injection of 0.275 mmol l^{-1} Co^{2+} yields a similar concentration. First, the sensitivity of the ERG responses to Co^{2+} was determined. Fig. 6A shows the ERG response for various stimulus intensities. The ERG response shape changed after application of cobalt (Fig. 6B). The A-wave was reduced and the B-wave was temporally broader. However, the intensity response relationship did not change appreciably (Fig. 6C), indicating that the sensitivity of the cones was not affected.

Sham injections of an equal volume of NaCl did not lead to significant change in response shape or sensitivity. Next we examined whether Co^{2+} changed the spectral sensitivity of the ERG. There were minor changes in spectral sensitivity after Co^{2+} injections, indicating that Co^{2+} slightly increased sensitivity in the shortwave spectrum and slightly decreased sensitivity in the longwave spectrum but since these changes were quite small, we conclude that Co^{2+} did not significantly affect any cone mechanism

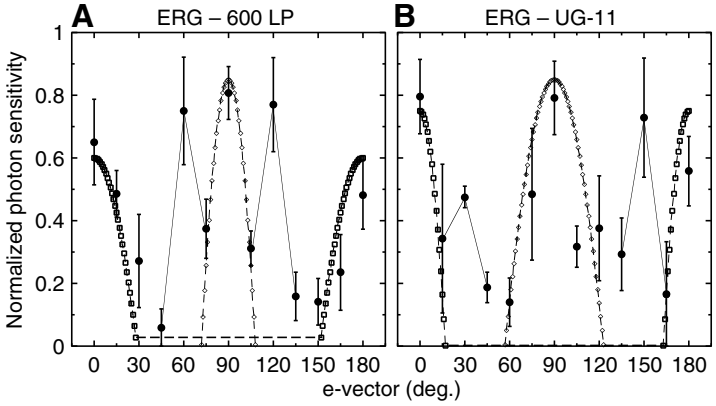

Fig. 5. Mean ultraviolet polarization sensitivity of rainbow trout (±1 standard error). (A) Electroretinogram (ERG) UV PS with LWS cone mechanism adaptation using the 600 nm long pass background (N=3). Note the intermediary peak shifts towards the horizontal polarization mechanism and the angular breadth of the horizontal polarization mechanism decreases while the vertical polarization mechanism increases. (B) ERG UV PS with UVS cone mechanism chromatic adaptation using a UG-11 background (N=3). Note the intermediary peaks shift towards the vertical polarization mechanism and the angular breadth of the horizontal polarization mechanism increases and the vertical decreases. S_v is represented by squares and S_h by diamonds. See Table 2 for linear subtractive model weighting functions.

specifically (Fig. 7). However, the polarization sensitivity was affected (Fig. 8). A low dose of Co^{2+} resulted in a complete collapse of the intermediate peaks. In this condition, both the ERG and the CAP had peaks at 0°, 90° and 180°. Sham injections did not change the tuning curve at all. Owing to the limited availability of fish we were not able to examine the effect of Co^{2+} on CAP polarization sensitivity.

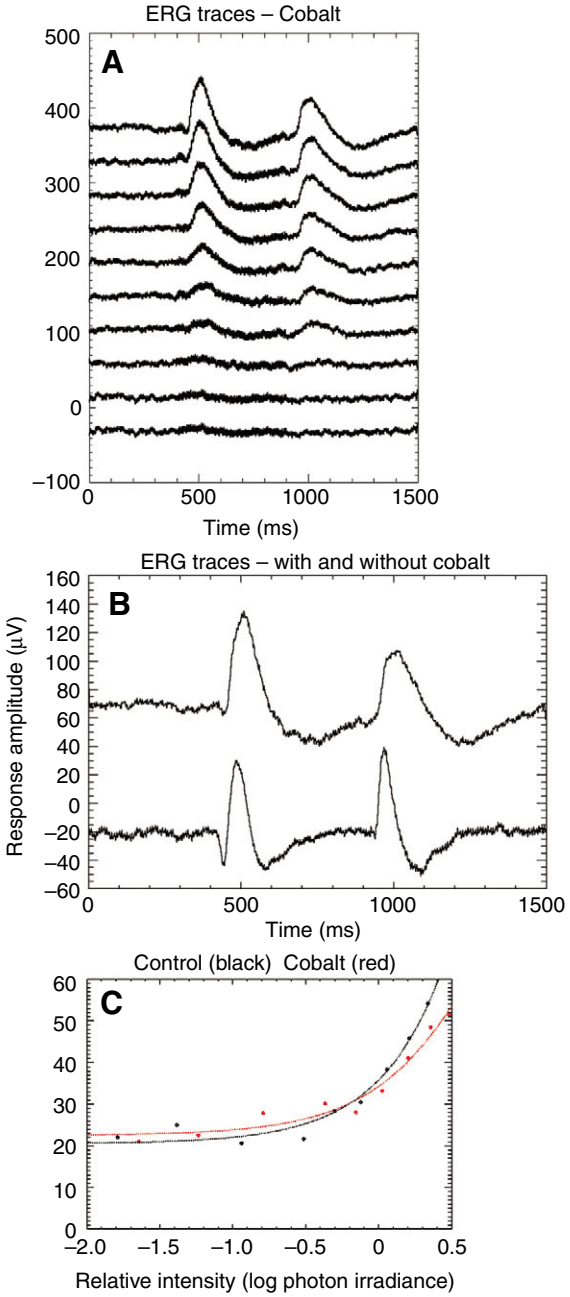

Fig. 6. Analysis of the effect of cobalt chloride on electroretinogram (ERG) responses. (A) ERG waveforms at increasing intensities recorded from a cobalt-treated fish (intraocular injection of cobalt chloride, intraocular concentration of 0.275 mmol l^{-1}). (B) Comparison of ERG waveforms from cobalt chloride-injected fish (upper trace) and the control (lower trace). (C) Response *versus* intensity based on ERG data taken from a cobalt chloride-injected fish and a control fish. The cobalt-injected fish show a lower slope in the dynamic range resulting in a difference in the interpolated threshold intensity.

DISCUSSION

Retinal information transfer of polarization is a product of network processing in the outer and inner retina. Polarization sensitivity in the outer retina, measured by ERG recording, reveals a response function with vertical and horizontal detector mechanisms in addition to intermediary peaks. Chromatic adaptation was used to manipulate the position of these intermediary peaks relative to the vertical or horizontal polarization detector mechanisms. For instance, UVS cone mechanism adaptation resulted in the displacement of the intermediary peaks towards the vertical detector mechanism. The width of the vertical detector peak decreased and that of the horizontal detector increased. LWS cone mechanism adaptation displaced the intermediary peaks towards the horizontal detector mechanism. The width of the vertical detector increased and that of the horizontal detector decreased. Both the shifts in the position of the intermediary peaks and the changes in the breadth of the polarization detector mechanisms argue strongly for the role of feedback processes in tuning polarization sensitivity in the outer retina. The interaction between cone mechanisms is mediated by negative feedback of the horizontal cells onto cones. We used intraocular injections of cobalt chloride to block this negative feedback and observed a dramatic reduction in the amplitude of intermediary peaks. Our study demonstrates the importance of horizontal cell feedback onto cones as a critical coding step or process that shapes the output of the vertical and horizontal polarization detector mechanisms. We will now turn our attention to how negative feedback of horizontal cells on cones could mediate opponent processes in polarization sensitivity.

Origin of Intermediary peaks: cobalt treatment and intermediary peaks

Our study revealed significant differences in the ERG waveform characteristics of control and cobalt chloride-treated test fish. For instance, the A-wave component was diminished in cobalt-treated fish in relation to the control. Recent studies have shown that cobalt treatment can block inward currents in rod photoreceptors, resulting in a suppression of signal transmission (Green and Kapousta-Bruneau, 1999; Yuan and Yang, 1997). Yuan and Yang (Yuan and Yang, 1997) suggest that cobalt-induced signal suppression results from a blockage of glutamate uptake by photoreceptors.

Cobalt is known to block horizontal cell-mediated feedback on cones in goldfish retina (Fahrenfort et al., 2004; Thoreson and Burkhardt, 1990). The result of blocking negative feedback of horizontal cells on cones is that the cone synapse is rendered out of its working range (Kamermans et al., 1998; Kamermans et al., 2001). Furthermore, blocking feedback of horizontal cells on cones will lead to a reduction of the high pass filter characteristics of the synapse. Consistent with this we observed a lower amplitude signal with a temporally broader B-wave. The broader B-wave suggests that blocking horizontal cell feedback with Co^{2+} treatment eliminates the high pass filtering characteristic of feedback. Cobalt treatment may have had other effects on the system. For instance, Co^{2+} could have an effect on cellular shutdown mechanisms in photoreceptors (e.g. arrestin and/or guanylyl cyclase) or as a recent study has shown, Co^{2+} could cause the production of hypoxia-induced factor-1 alpha in retinal pigment epithelial cells (Wang et al., 2005). This possibility would be comparable to mimicking hypoxic conditions in the retinal pigment epithelium, thus suppressing the C-wave. However, the finding that the D-wave component had reduced amplitude and a temporally broader response strongly suggests that Co^{2+} reduced horizontal feedback. Thus, the implications of these other cobalt effects for our study would seem to be rather limited.

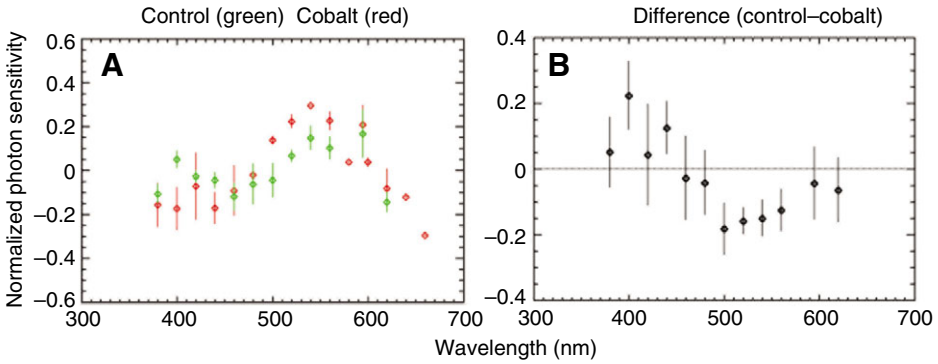

Fig. 7. Mean normalized spectral sensitivity (±1 standard error). (A) Sensitivity of control fish in green (N=3) and cobalt chloride-treated fish (estimated intraocular concentration was 0.275 mmol l^{-1}; N=3) in red. (B) Mean difference spectrum (control minus treated).

As discussed previously, sub-millimolar concentrations of Co^{2+} inhibit feedback from horizontal cells to cones. Intraocular concentrations of 0.275 mmol l^{-1} Co^{2+} resulted in significant attenuation or elimination of the intermediary peaks. The intermediary peaks appear to function as feedback activity, and that significant reduction in horizontal cell feedback results in the two channels being expressed primarily in the feed-forward pathways.

To support the hypothesis that the intermediary peaks are the result of feedback of horizontal cells on cones, we need to identify a feed-forward signal that generates the ON-bipolar response that is reduced when feedback is reduced. Our results suggest that such a reduction in feed-forward signals occurs in both the chromatic adaptation conditions and the Co^{2+} treatments. During the UVS cone adaptation and Co^{2+} treatments, there is a relative reduction in the UVS cone mechanism feed-forward signal due to the reduction in feedback of horizontal cells onto the LWS/horizontal detector. The LWS cone mechanism adaptation condition resulted in a relative reduction in inhibitory feedback onto the UVS cones, resulting in a relatively smaller feed-forward signal from the LWS/horizontal detector mechanism compared to the other conditions.

Potential mechanisms for the generation of intermediary peaks

UV polarization vision in teleosts is dependent on the presence of two differentially sensitive polarization detectors. These detectors are represented by different spectral classes of cones in the case of rainbow trout: the vertical detector mediated by the UVS cones and the horizontal detector by the MWS/LWS double cones. How are the intermediary peaks generated?

First, we need to consider interactions between different spectral classes of cones, for example, MWS/LWS members of double cones, and UVS/LWS cones evident at the horizontal cell level and at higher levels in the visual pathway of salmonid fishes (Coughlin and Hawryshyn, 1995; Nakano et al., 2006). Second, colour-coded neurons in the torus semicircularis that show UV polarization sensitivity are always UV on/red off (Coughlin and Hawryshyn, 1995). Third, chromatic adaptation using a UV or a long wavelength background results in changes in UV polarization sensitivity such as shifting the position of intermediary peaks and increasing or decreasing the width of the horizontal and vertical detector mechanism peaks.

It is clear from our experiments that cobalt blocks negative feedback of horizontal cells on cones, and that the modulation of polarization sensitivity comes principally through this feedback. The evidence from both the chromatic adaptation and cobalt treatment suggests that the outcome of the MWS/LWS opponent interaction (horizontal detector) influences the negative feedback of horizontal cells onto UVS cones and that UVS cones feedback to MWS/LWS cones through negative feedback from horizontal cells. At an e-vector orientation of 45° or 135°, the opponent interaction of MWS/LWS cones reduces the negative feedback on UVS cones, thus producing the intermediary peaks. Chromatic adaptation changes the balance of interaction between the vertical and horizontal detector mechanisms and thus if either detector dominates, it pushes the intermediary peak towards the depressed detector and it narrows the width of sensitivity of the depressed detector. The outcome of these interactions sets the output of the outer retina.

In addition, studies on turtle retina have shown that cone–cone coupling can lead to the LWS cone mechanism providing excitatory input to shortwave-sensitive cone mechanisms (Itzhaki et al., 1992). Cone–cone coupling could enhance sensitivity if two differentially sensitive photoreceptor mechanisms were stimulated in a zone of overlapping sensitivity [spectral or polarization (O'Brien et al., 2004)]. Although this aspect of retinal function has not been

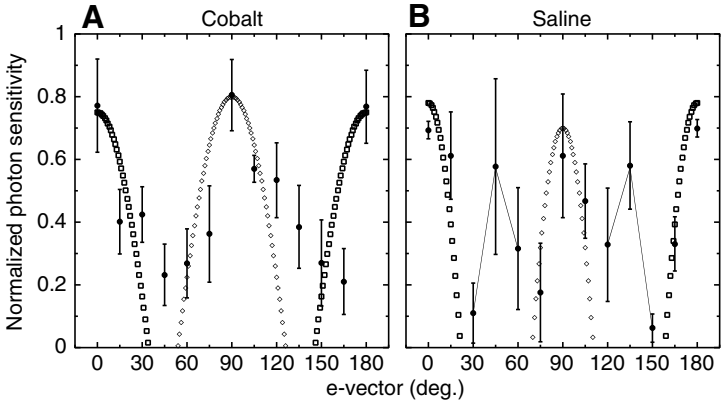

Fig. 8. Mean normalized ultraviolet polarization sensitivity of rainbow trout (±1 standard error). (A) Electroretinogram (ERG) UV PS of fish treated with cobalt chloride (intraocular concentration ~0.275 mmol l^{-1}; N=3). (B) Sham control intraocular injection of saline (N=3). S_v is represented by squares and S_h by diamonds. See Table 2 for linear subtractive model weighting factors.

examined for rainbow trout, it could represent an additional mode of retinal processing in polarization vision.

Work on insect polarization sensitivity suggests that antagonistic interaction of polarization detectors, through opponency, has features comparable to what we see in fish retina. Labhart and Meyer (Labhart and Meyer, 2002) suggest that POL neurons in the optic lobe of crickets receive input from differentially sensitive polarization detectors that operate in an opponent manner for purposes of signal conditioning. They indicate that polarization opponency functions to enhance e-vector contrast for effective coding at low degrees of polarization, and it moderates neuronal sensitivity to variations in ambient intensity focusing activity on coding differential polarization detector input.

Do spectral confounds interfere with polarization sensitivity?

Research to date indicates that spectral confounds are minimized by the coincidence of spectral absorption of UVS and MWS/LWS cones in the UV portion of the spectrum. Thus UV linearly polarized light stimulates the α-band absorption of the UVS cones and the β-band absorption of the MWS/LWS cones, two orthogonally sensitive polarization detectors (see Parkyn and Hawryshyn, 1993). It is important to note, however, that the issue of spectral confounds requires serious examination since stimulation of the MWS and/or LWS cone mechanism could lead to a spectral signal of sufficient strength to confound the polarization stimulus. However, our data argue strongly against this possibility. (1) Recordings from retinal neurons (largely retinal ganglion cells), performed to test for UV polarization sensitivity, always show distinct vertical and horizontal polarization detector mechanisms (Parkyn and Hawryshyn, 1993; Parkyn and Hawryshyn, 2000). A spectral confound would have the effect of showing either the horizontal detector mechanism dominating the polarization sensitivity or polarization sensitivity disappearing because the spectral signal becomes the salient feature. (2) Test fish that have been shown to have UVS cone loss from the central and ventral retina through programmed cell death (Allison et al., 2003; Allison et al., 2006), show polarization sensitivity with only the horizontal detector mechanism present (Hawryshyn, 2000). (3) Recordings from neurons in the torus semicicularis (mid brain structure) show similar characteristics of polarization sensitivity to retinal neurons (Coughlin and Hawryshyn, 1995). (4) Behavioural studies show that the UV content in linearly polarized stimuli is essential for e-vector spatial orientation and e-vector discrimination behaviour (Degner and Hawryshyn, 2001; Hawryshyn et al., 1990; Mussi et al., 2005; Parkyn et al., 2003). If the UV spectrum is eliminated from the linearly polarized stimulus with a UV cut-off filter or the UVS cones have disappeared in the central and ventral retina, salmonid test fish are incapable of responding to the polarization stimulus (Hawryshyn at al., 1990; Mussi et al., 2005). Spectral confounds would distort or detrimentally affect e-vector spatial orientation and discrimination.

So we conclude that spectral confounds play a relatively insignificant role in interfering with polarization sensitivity.

Behavioural relevance of feedback interactions in the retina

The current study on rainbow trout along with examination of damselfish (green chromis) (Hawryshyn et al., 2003) polarization sensitivity, indicate that these two species have similar polarization processing in the outer retina. We have recently used green chromis in behavioural studies examining polarization discrimination. Green chromis appear to have very good polarization discrimination capabilities; easily differentiating horizontal and vertical planes of linearly polarized light independent of brightness (Mussi et al., 2005). The capacity for e-vector discrimination disappeared when the UV portion of the light stimuli was filtered out, indicating that the presence of UV polarized light is critical for e-vector discrimination. In addition, damselfish were able to distinguish between relatively small e-vector orientations of polarized light with the minimum separable e-vector of 15°–25°. The discriminative performance of *C. viridis* was greatest at e-vector orientations close to or at the point of maximum overlapping sensitivity of the two polarization detector mechanisms. Thus polarization discrimination appears to be at its optimal level of performance when the two detector mechanisms are interacting through interneuronal processing mediated by horizontal cells.

We have used rainbow trout in a related discrimination paradigm (Degner and Hawryshyn, 2001). A notable difference was that trout were not capable of polarization discrimination on a horizontal line of sight. Rather trout could perform discriminations on a downwelling projection of the polarization field. This difference in polarization discriminative behaviour between species could be a good indication of the functional utility of polarization vision in fishes. Damselfish are strongly zooplanktivous, so one possible function of polarization vision in damselfish could be the enhancement of contrast between the zooplankter and background veiling radiance. In rainbow trout, however, discriminative resolution of the e-vector is much poorer (Degner and Hawryshyn, 2001) and thus not as likely to be related to plankton feeding, but more likely to be crucial for navigation (Parkyn et al., 2003).

Despite the differences in functionality, negative feedback interactions between horizontal cells and cones modulates or shapes the feed forward polarization signal through the retina. The commonality seen in polarization sensitivity between species would suggest that this information processing is probably an important and general feature in polarization vision.

We thank the Fraser Valley Trout Hatchery, Abbottsford, British Columbia, Canada for supplying the fish. This research was supported by an operating grant (grant number F49620-01-0560, PI: C.W.H.) from the US Air Force Office of Scientific Research BioInspired Program. The experiments described in this paper comply with the “Principles of animal care”, publication 86-23, revised 1985 of the National Institute of Health and also with the University of Victoria, Animal Care Committee under the auspices of the Canadian Council on Animal Care. We thank Drs Chengfeng Xiao and Suzanne Gray for comments on the manuscript. C.W.H. is supported by the Canada Research Chair program.

REFERENCES

Allison, W. T., Dann, S. G., Helvik, J. V., Bradley, C., Moyer, H. D. and Hawryshyn, C. W. (2003). Ontogeny of ultraviolet-sensitive cones in the retina of rainbow trout (*Oncorhynchus mykiss*). *J. Comp. Neurol.* **461**, 294-306.

Allison, W. T., Dann, S. G., Veldhoen, K. M. and Hawryshyn, C. W. (2006). Degeneration and regeneration of ultraviolet cone photoreceptors during development in rainbow trout. *J. Comp. Neurol.* **499**, 702-715.

Barry, K. L. and Hawryshyn, C. W. (1999). Spectral sensitivity of the Hawaiian saddle wrasse, *Thalassoma duperrey*, and implications for visually mediated behaviour on coral reefs. *Environ. Biol. Fishes* **56**, 429-442.

Beaudet, L., Browman, H. I. and Hawryshyn, C. W. (1993). Optic-nerve response and retinal structure in rainbow-trout of different sizes. *Vision Res.* **33**, 1739-1746.

Brown, K. T. (1968). The electroretinogram: its components and their origin. *Vision Res.* **8**, 633-677.

Coughlin, D. J. and Hawryshyn, C. W. (1995). A cellular basis for polarized-light vision in rainbow-trout. *J. Comp. Physiol. A* **176**, 261-272.

Cronin, T. W. and Shashar, N. (2001). The linearly polarized light field in clear, tropical marine waters: spatial and temporal variation of light intensity, degree of polarization and e-vector angle. *J. Exp. Biol.* **204**, 2461-2467.

Degner, S. and Hawryshyn, C. W. (2001). Orientation of rainbow trout (*Oncorhynchus mykiss*) to linearly polarised light fields. *Can. J. Zool.* **79**, 407-415.

Delius, J. D., Perchard, R. J. and Emmerton, J. (1976). Polarized-light discrimination by pigeons and an electroretinographic correlate. *J. Comp. Physiol. Psychol.* **90**, 560-571.

DeMarco, P. J., Jr and Powers, M. K. (1989). Sensitivity of ERG components from dark-adapted goldfish retinas treated with APB. *Brain Res.* **482**, 317-323.

Fahrenfort, I., Sjoerdsma, T., Ripps, H. and Kamermans, M. (2004). Cobalt ions inhibit negative feedback in the outer retina by blocking hemichannels on horizontal cells. *Vis. Neurosci.* **21**, 501-511.

Green, D. G. and Kapousta-Bruneau, N. V. (1999). A dissection of the electroretinogram from isolated rat retina with microelectrodes and drugs. *Vis. Neurosci.* **16**, 727-741.
Hawryshyn, C. W. (1991). Light-adaptation properties of the ultraviolet-sensitive cone mechanism in comparison to the other receptor mechanisms of goldfish. *Vis. Neurosci.* **6**, 293-301.
Hawryshyn, C. W. (2000). Ultraviolet polarization vision in fishes: possible mechanisms for coding e-vector. *Philos. Trans. R. Soc. Lond. B Biol. Sci.* **355**, 1187-1190.
Hawryshyn, C. W. and McFarland, W. N. (1987). Cone photoreceptor mechanisms and the detection of polarized light in fish. *J. Comp. Physiol. A* **160**, 459-465.
Hawryshyn, C. W., Arnold, M. G., Bowering, E. and Cole, R. L. (1990). Spatial orientation of rainbow-trout to plane-polarized light-the ontogeny of e-vector discrimination and spectral sensitivity characteristics. *J. Comp. Physiol. A* **166**, 565-574.
Hawryshyn, C. W., Moyer, H. D., Allison, W. T., Haimberger, T. J. and McFarland, W. N. (2003). Multidimensional polarization sensitivity in damselfishes. *J. Comp. Physiol. A* **189**, 213-220.
Hzn, J. J. V., Coemans, M. A. J. M. and Nuboer, J. F. W. (1995). No evidence for polarization sensitivity in the pigeon electroretinogram. *J. Exp. Biol.* **198**, 325-335.
Itzhaki, I., Malik, S. and Perman, I. (1992). Spectral properties of short-wavelength (blue) cones in the turtle retina. *Vis. Neurosci.* **9**, 235-241.
Joly, D. W., Mawdesley-Thomas, L. E. and Bucke, D. (1972). Anaesthesia of fish. *Vet. Rec.* **91**, 424-426.
Kamermans, M., Kraaij, D. A. and Spekreijse, H. (1998). The cone/horizontal cell network: a possible site for color constancy. *Vis. Neurosci.* **15**, 787-797.
Kamermans, M., Kraaij, D. and Spekreijse, H. (2001). The dynamic characteristics of the feedback signal from horizontal cells to cones in the goldfish retina. *J. Physiol. Lond.* **534**, 489-500.
Kreithen, M. L. and Keeton, W. T. (1974). Detection of polarized-light by homing pigeon, *Columba livia*. *J. Comp. Physiol.* **89**, 83-92.
Labhart, T. and Meyer, E. P. (2002). Neural mechanisms in insect navigation: polarization compass and odometer. *Curr. Opin. Neurobiol.* **12**, 707-714.
McFarland, W. and Munz, F. W. (1975a). Part II. The photic environment of clear tropical seas during the day. *Vision Res.* **15**, 1063-1070.
McFarland, W. and Munz, F. W. (1975b). Part III. The evolution of photopic visual pigments in fishes. *Vision Res.* **15**, 1071-1080.
Mussi, M., Haimberger, T. J. and Hawryshyn, C. W. (2005). Behavioural discrimination of polarized light green chromis (*Chromis viridis*). *J. Exp. Biol.* **208**, 3037-3046.
Nakano, N., Kawabe, R., Yamashita, N., Hiraishi, T., Yamamoto, K. and Nashimoto, K. (2006). Color vision, spectral sensitivity, accommodation, and visual acuity in juvenile masu salmon *Oncorhynchus masou masou*. *Fish. Sci.* **72**, 239-249.
Novales Flamarique, I. and Hawryshyn, C. W. (1993). Spectral characteristics of salmonid migratory routes from southern Vancouver Island (British Columbia). *Can. J. Fish. Aquat. Sci.* **50**, 1706-1716.
Novales Flamarique, I. and Hawryshyn, C. W. (1997). Is vertebrate use of underwater polarized light restricted to crepuscular time periods? *Vision Res.* **37**, 975-989.
Novales Flamarique, I., Hawryshyn, C. W. and Harosi, F. I. (1998). Double-cone internal reflection as a basis for polarization detection in fish. *J. Opt. Soc. Am. A* **15**, 349-358.
O'Brien, J., Nguyen, H. B. and Mills, S. L. (2004). Cone photoreceptors in bass retina use two connexins to mediate electrical coupling. *J. Neurosci.* **24**, 5632-5642.
Parkyn, D. C. and Hawryshyn, C. W. (1993). Polarized-light sensitivity in rainbow trout (*Oncorhynchus mykiss*): characterization from multi-unit responses in the optic nerve. *J. Comp. Physiol. A* **172**, 473-500.
Parkyn, D. C. and Hawryshyn, C. W. (2000). Spectral and ultraviolet-polarisation sensitivity in juvenile salmonids: a comparative analysis using electrophysiology. *J. Exp. Biol.* **203**, 1173-1191.
Parkyn, D. C., Austin, J. D. and Hawryshyn, C. W. (2003). Acquisition of polarized-light orientation in salmonids under laboratory conditions. *Anim. Behav.* **65**, 893-904.
Pomozi, I., Horvath, G. and Wehner, R. (2001). How the clear-sky angle of polarization pattern continues underneath clouds: full sky measurements and implications for animal orientation. *J. Exp. Biol.* **204**, 2933-2942.
Roberts, N. W. and Needham, M. G. (2007). A mechanism of polarized light sensitivity in cone photoreceptors of the goldfish (*Carassius auratus*). *Biophys. J.* **93**, 3241-3248.
Roberts, N. W., Gleeson, H. E., Temple, S. E., Haimberger, T. J. and Hawryshyn, C. W. (2004). Differences in the optical properties of vertebrate photoreceptor classes leading to axial polarization sensitivity. *J. Opt. Soc. Am. A* **21**, 335-345.
Shashar, N. and Cronin, T. W. (1996). Polarization contrast vision in *Octopus*. *J. Exp. Biol.* **199**, 999-1004.
Shashar, N. and Hanlon, R. T. (1997). Squids (*Loligo pealei* and *Euprymna scolopes*) can exhibit polarized light patterns produced by their skin. *Biol. Bull.* **193**, 207-208.
Shashar, N., Hanlon, R. T. and Petz, A. D. (1998). Polarization vision helps detect transparent prey. *Nature* **393**, 222-223.
Shashar, N., Borst, D. T., Ament, S. A., Saidel, W. M., Smolowitz, R. M. and Hanlon, R. T. (2001). Polarization reflecting iridophores in the arms of the squid *Loligo pealeii*. *Biol. Bull.* **201**, 267-268.
Thoreson, W. B. and Burkhardt, D. A. (1990). Effects of synaptic blocking agents on the depolarizing responses of turtle cones evoked by surround illumination. *Vis. Neurosci.* **5**, 571-583.
Vigh, J. and Witkovsky, P. (1999). Sub-millimolar cobalt selectively inhibits the receptive field surround of retinal neurons. *Vis. Neurosci.* **16**, 159-168.
Wang, B., Li, H., Yan, H. and Xiao, J. G. (2005). Genistein inhibited hypoxia-inducible factor-1 alpha expression induced by hypoxia and cobalt chloride in human retinal pigment epithelium cells. *Methods Find. Exp. Clin. Pharmacol.* **27**, 179-184.
Waterman, T. H. and Hashimoto, H. (1974). E-vector discrimination by goldfish optic tectum. *J. Comp. Physiol.* **95**, 1-12.
Yuan, L. L. and Yang, X. L. (1997). Selective suppression of rod signal transmission by cobalt ions of low levels in carp retina. *Sci. China C Life Sci.* **40**, 128-136.